A STUDY OF THE THERMAL EVOLUTION OF MARS VIA VISCOELASTIC RELAXATION OF LARGE CRATERS. M. Karimi[1], A.J. Dombard[1], and R.M. Williams[2], [1]Dept. of Earth and Environmental Sciences, Univ. of Illinois at Chicago, 845 W. Taylor St. (MS-186), Chicago, IL 60607 (mkarim5@uic.edu), [2]Planetary Science Institute, 1700 East Fort Lowell, Suite 106, Tucson, AZ 85719.

Introduction: Internal heat transfer drives the geological evolution of a planet, and gaining a better understanding of thermal history plays an important role in planetary studies. Since the direct measurement of the heat flux on Mars has not been yet possible, an indirect method must be employed. Because the thickness of the mechanical lithosphere is strongly sensitive to interior temperatures, simulation of lithospheric deformation is an appropriate method for studying the heat flux of Mars. Previous lithospheric modeling studies focused on specific geographic areas like the giant volcanoes at Tharsis [1] or on specific features like rift systems [2], the Crustal Dichotomy [3, 4, 5], wrinkle ridges [6], and polar caps [7]. By covering limited geography and/or limited time spans, these studies have provided a narrow and incomplete understanding of the planet's thermal history. For example, each of the above features only represents a small part of the total surface area of the planet.

Here, we constrain the heat flux of Mars by simulating the surface and subsurface viscoelastic deformation of large Martian craters due to lower crustal flow [8]. Studies of Martian crustal thickness revealed that the mantle is often uplifted beneath large craters [e.g., 9], likely during collapse of the transient crater. High temperatures in the lower crust accompanied by a pressure gradient due to crustal thickness variations may have caused the lower crust to flow [e.g., 10]. Lateral flow of the lower crust transfers the material from the periphery and thickens the crust beneath the crater, thus causing the time-dependent reduction of the topography at the crust/mantle boundary (CMB). Loss of isostatic support results in a transition of support of surface topography from buoyancy to lithospheric strength [8]. This process is a function of the flow channel thickness [10] and the lower crust viscosity, and thus this phenomenon is very sensitive to background heat flux [8]. Furthermore since this process requires the presence of remnant impact heat [8], it occurs in the epoch immediately following the impact. Since the formation of the impact craters spans the planet's history, and since the impacts are distributed roughly uniformly over the surface, a study of large craters can provide a more complete spatial and temporal view of the thermal evolution of the planet.

Methods: The craters in this analysis are ~200-500 km in diameter, large enough to be resolved in current gravity models yet small enough to avoid craters with complex histories (e.g., Hellas). This study focuses on 15 craters, 11 of which date to the middle Noachian as determined from a geologic map by Skinner et al. [11]. Of the remaining 4, there is 1 each from the Hesperian and late Noachian, and two from the early Noachian.

Using the *MSC.Marc* finite element package, an axisymmetric mesh is employed to simulate the evolution of the surface and CMB of these large craters. The shape of the initial crater is a 4^{th} order polynomial depression flanked by an inverse 3^{rd} power ejecta blanket [12]. All of our candidate craters are far shallower than predicted from an extrapolation of depth-diameter curves [13], yet despite this, the craters all appear strongly under-compensated [8]. Thus our initial rim-to-floor depths follow the depth-diameter trends of Boyce and Grabeil [13], though we also consider an initial depth limited by our deepest candidate crater (the Hesperian aged Newton). Initial rim heights are constrained by Garvin et al. [14]. We assume that all craters begin in Airy isostatic balance in a crust 50 km thick (density of 2900 kg m^{-3}) over a mantle (density of 3500 kg m^{-3}). Our meshes typically have of order 10^4 elements. The selected craters are subjected to an uncoupled thermomechanical analysis, in which a thermal solution is piped into a mechanical solution.

Thermal solution. We perform a steady state thermal simulation in which the surface temperature is fixed at 210 K, with an applied basal heat flux and zero heat flux on the sides. In order to approximate the impact heat, we constrain the temperature of the uplifted CMB beneath the crater to that of the undeflected boundary. Thermal conductivities of the crust and mantle are 2.5 and 4 W m^{-1} K^{-1}, respectively.

Mechanical solution. The mechanical simulations are run over a time scale of 100 Myr, the approximate diffusion time of the remnant impact heat. The boundary conditions are fixed-nodes on the base, free slip on the sides, and a vertical gravity load with an acceleration of 3.7 m s^{-2}. The nominal elastic Young modulus and Poisson's ratio for the crust are 65 GPa and 0.25, and 140 GPa and 0.25 for the mantle [15]. The viscous rheology of the crust follows that of a wet Maryland diabase [16], while the mantle's rheology follows the flow law of a wet natural peridotite [17]. To keep the computer times tractable (days to weeks), we limit the minimum viscosity within the mesh to 10^{21} Pa s.

Results: We compare our predicted topography on the CMB against that from a model of crustal thickness

on Mars, as determined by simultaneous analysis of the gravity and topography [9,18]. (Though it is considered, we are less concerned about the evolution of the surface topography, because of the potential for post-impact crater fill.) We attempt to find the magnitude of the background heat flux that best predicts this subsurface topography. The results of our simulations show that a typical heat flux for the craters from the early Noachian is ~70-75 mW m^{-2} (assuming an initially deep crater), and ~60-65 mW m^{-2} (for shallow craters). For the craters from the mid-Noachian, the heat flux values range from 50-75 mW m^{-2} (deep craters) to 45-65 mW m^{-2} (shallow craters). Our simulations show that for late Noachian terrain, the heat flux values are 45-50 mW m^{-2} (deep) to 45 mW m^{-2} (shallow). The best-matching simulation of Newton Crater, located in Hesperian terrain and the least deformed candidate, shows a heat flux value less than 45 mW m^{-2} for both deep and shallow structures, which is indicative of a reduced heat flux in the Hesperian.

Since the geographical location of the craters varies, surface temperature might differ from the average value used in this study. Therefore in order to test for any variations, we also perform simulations over a range of surface temperatures (180 to 230 K). Our study shows that the sensitivity of the results to surface temperature is not significant; best-matching heat flows only vary by at most 7%.

Discussion: Among these craters, 11 of them are dated mid-Noachian. Best-matching simulations reveal a regional variation in heat flux, with higher values closer to the boundary of the Crustal Dichotomy. Since the mid-Noachian covers a relatively short time period (~100 Myr), this variation is not likely due to secular cooling of the planet. Instead, these results suggest that the process that formed the Dichotomy still had a thermal signature in the mid-Noachian (Fig. 1). This conclusion is not sensitive to choices made for our simulations (e.g., our value of the minimum viscosity), because the craters closer to the boundary have less CMB topography (which is what necessitated the higher heat flux values in our simulations).

Looking beyond the mid-Noachian, our simulations seem to chart the secular cooling of Mars, with higher heat fluxes needed for older (and more deformed) craters. Indeed, Newton Crater is the youngest and hence least deformed crater, which explains the lower heat flux value needed to match its CMB topography. Figure 2 summarizes our heat flux values along with a review of different thermal histories of Mars [19]. Our assessed heat flux values are slightly on the high side-though still within the range of the predicted values from Martian thermal models.

References:[1] Comer R.P. et al. (1985) *Rev. Geophys., 23*, 61-92. [2] Anderson F.S. and Grimm R.E. (1998) *JGR, 103*, 11113-11124. [3] McGovern P.J. et al. (2002) *JGR, 107*, 5136. [4] McGovern P.J. et al. (2004) *JGR*, 109, E07007. [5] Watters T. R. and McGovern P. J. (2006) *Geophys. Res. Lett, 33*, L08S05. [6] Montesi L.G.J. and Zuber M.T. (2003) *JGR*, 108, 5048. [7] Dombard A.J. and Phillips R.J. (2010) *LPS XXXVI*, abstract #1878. [8] Karimi M. and Dombard A.J. (2011) *AGU fall meeting*, abstract #P43D-1712. [9] Neumann G.A. et al. (2004) *JGR, 109*, E08002. [10] Nimmo F. and Stevenson D.J. (2001) *JGR, 106*, 5085-5098. [11] Skinner, J. A. (2006) *LPS XXXVII*, abstract #2331. [12] Dombard A.J. and McKinnon W.B. (2006) *JGR*, *111*, E01001. [13] Boyce J.M. and Grabeil H. (2007) *Geophys. Res. Lett*., *34*, doi:10.1029/2007GL029731. [14] Garvin J.B. et al. (2003), *6th Inter. Conf. Mars*, abstract #3277. [15] Turcotte D.L. and Schubert G. (2002) *Geodynamics*, Cambridge U. Press. [16] Caristan Y. (1982) *JGR*, *87*, 6781-6790. [17]Karato S.-I. and Wu P. (1993) *Science*, *260*, 771-778. [18] Neumann G.A. et al. (2008) *LPS XXXIX*, abstract #2167. [19] Solomon S.C. et al. (2005) *Science*, *307*, 1214-1220.

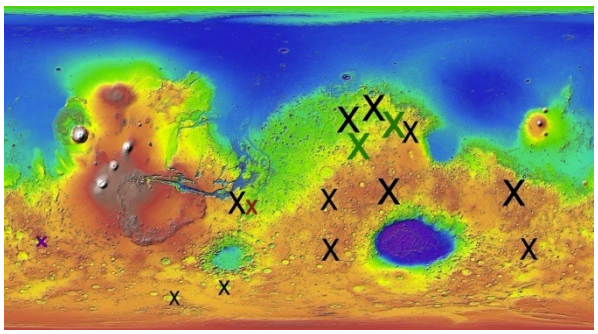

Figure 1. A topographic map of Mars with the locations of our candidate craters. Green, black, red, and purple signs are indicative of early Noachian, mid-Noachian, late Noachian, and Hesperian. The size of the symbol is related to the background heat flux.

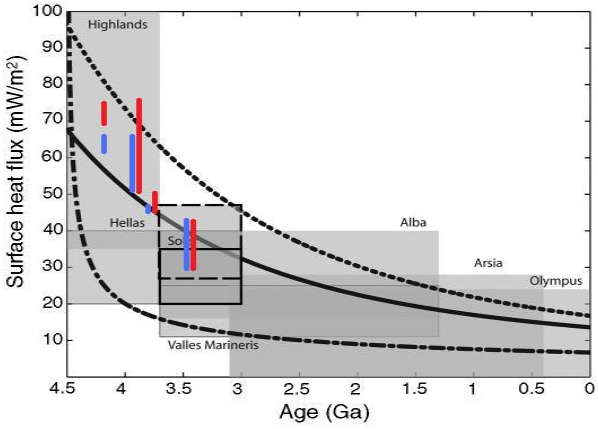

Figure 2. Estimation of Martian heat flux versus time combined with our results, modified from [19]. Blue and red bars show ranges from our initially shallow and deep craters, respectively.